Molecular BioSystems

RSC Publishing

PAPER

View Article Online
View Journal | View Issue

Cite this: *Mol. BioSyst.*, 2013, **9**, 492

Sequential selective enrichment of phosphopeptides and glycopeptides using amine-functionalized magnetic nanoparticles

Ying Zhang,[ab] Huijie Wang*[a] and Haojie Lu*[ab]

Received 19th July 2012,
Accepted 3rd January 2013

DOI: 10.1039/c2mb25288k

www.rsc.org/molecularbiosystems

As two of the most common and important post-translational modifications (PTMs) of proteins, glycosylation and phosphorylation play critical roles in biological processes. Because of the low abundance of phosphopeptides/glycopeptides, specific and sensitive strategies are especially indispensable for the identification of protein phosphorylation and glycosylation by mass spectrometry (MS). However, most of those previously reported methods only focused on enriching either phosphopeptides or glycopeptides rather than enriching both of them. In the present study, amine-functionalized magnetic nanoparticles were synthesized in a one-pot procedure and successfully used for selective enrichment of both phosphopeptides and glycopeptides. The selectivity of this method was demonstrated by analyzing the mixture of peptides/phosphopeptides/glycopeptides at molar ratio of 10 : 1 : 1; the post-enrichment recovery was 88% and 76% for phosphopeptides and glycopeptides respectively. The sensitivity was at the fmol level for both of the phosphopeptides and glycopeptides. In addition, sequence coverage was increased from 25.6% to 51.8% corresponding to a 102% increase for a model protein asialofetuin. These newly identified phosphopeptides or glycopeptides provided additional sequence information, which was beneficial to the protein identification.

Introduction

Glycosylation and phosphorylation are two of the most common and important post-translational modifications (PTMs) of proteins.[1] As a key regulator of intracellular biological processes, phosphorylation is known to be involved in the regulation of diverse processes including metabolism, transcriptional *etc*.[2] Glycosylation, another important PTM, is also of ultimate importance in many phenomena of physiology, such as cell development, cell division, tumor immunology *etc*.[3] Despite their ubiquitous roles, phosphoproteins and glycoproteins are generally present at relatively low abundance within the cell. Mass spectrometry (MS) is the most powerful technique for deciphering the phosphorylation[4] and glycosylation profiles of proteins nowadays.[5] However, characterizing these two PTMs is still a challenge with the state-of-art MS-based strategies.[6]

Because of their low abundances (less than 5% of the peptides in a typical complex protein digest are glycosylated[7] or phosphorylated[8]), MS responses of phosphopeptides/glycopeptides are always severely suppressed by nonphosphopeptides and nonglycopeptides. Therefore, selective enrichment of phosphopeptides and glycopeptides prior to MS analysis plays a very important role in the phosphoproteome and glycoproteome study. Various methods have been developed for phosphopeptide enrichment,[9] including immobilized metal ion affinity chromatography (IMAC) incorporating Ti^{4+},[10] Zr^{4+},[11] or Fe^{3+},[12] metal oxide affinity chromatography (MOAC) with TiO_2,[13] ZrO_2,[14] Al_2O_3[15] and Fe_3O_4,[16] interaction with positively charged substrates such as polyarginine (PA)–nanodiamond[17] or polyethylenimine-modified magnetic nanoparticles,[18] immunoprecipitation with phosphoprotein-specific antibodies,[19] and the addition of an affinity tag to phosphorylated amino acids through chemical reactions.[20] In order to enrich glycopeptides, methods based on lectin affinity chromatography,[21] hydrazine chemistry,[22] boronic acid-functionalized particles[23] and hydrophilic interaction liquid chromatography (HILIC)[24] have been developed. However, most of these strategies considered phosphopeptides or glycopeptides separately. As a result, glycopeptides are always lost in a phosphopetide enrichment procedure and *vice versa*. In mammals, it has been estimated that nearly 50% of all proteins are glycosylated,[25] and recent large scale phosphoproteomic studies

[a] *Shanghai Cancer Center, Fudan University, Shanghai 200032, P. R. China. E-mail: wanghj98@hotmail.com*
[b] *Institutes of Biomedical Sciences and Department of Chemistry, Fudan University, Shanghai 200032, P. R. China. E-mail: luhaojie@fudan.edu.cn*

suggested that more than half of all eukaryotic proteins are phosphorylated.[26] Some of the proteins were reported harboring both phosphorylation and glycosylation sites, for example, the full-length insulin-like growth factor-binding protein-5 (IGFBP-5), 27% of which is glycosylated and more than half of which is also monophosphorylated. Therefore, comprehensive, highly sensitive and specific enrichment strategies are needed in order to simultaneously characterize phosphorylation and glycosylation in a certain protein. Recently, titanium dioxide (TiO_2) has been reported for simultaneous enrichment of glycopeptides and phosphopeptides.[24] Phosphopeptides were captured by TiO_2 because unsaturated titania(IV) ions are strong Lewis acid with an affinity for compounds that donate electron pairs, allowing them to trap phosphopeptides. Glycopeptides were captured through hydrophilic interaction between glycan chains and TiO_2. Phosphopeptides and glycopeptides were then eluted with different elutions step-by-step. This method was proved successfully with the mixtures of the phosphoprotein alpha-casein (α-casein), glycoprotein horseradish peroxidase (HRP) and human serum albumin (HSA) (molar ratio 1 : 1 : 1). However, the selectivity and sensitivity are still unsatisfactory, and the preparation of TiO_2 microspheres is relative difficult. In the present study, we established a sequential selective enrichment method for phosphopeptides and glycopeptides using amine-functionalized magnetic nanoparticles (Fe_3O_4@NH_2) which were prepared in a facile one-pot synthesis procedure. Through the bridging bidentate binding formed between the phosphate anions and the Fe_3O_4 as well as the electrostatic interaction between negatively charged phosphate groups on phosphopeptides and positively charged Fe_3O_4@NH_2, phosphopeptides were selectively enriched. Glycopeptides were enriched by hydrophilic interactions between glycan chains and Fe_3O_4@NH_2 in a mostly organic solution, from the flow-through part after phosphopeptide enrichment. The whole enrichment procedure can be completed in less than 10 min. Mass spectrometric analysis revealed the selectivity and efficiency of this approach by analyzing phosphopeptides and glycopeptides in the digest mixture of beta-casein (β-casein), HRP and myoglobin (Myo) with molar ratio of 1 : 1 : 10. This approach was then used to analyze the tryptic digest of asialofetuin from bovines (ASF, a glycoprotein with predicted phosphorylated sites), and its phosphorylated sites were confirmed by experiments for the first time. Overall, this sequential enrichment strategy offers a simple and effective method for enrichment both of the phosphopeptides and glycopeptides step-by-step prior to MS analysis.

Experimental

Reagents and materials

2,5-Dihydroxybenzoic acid (2,5-DHB, 98%), α-cyano-4-hydroxycinnamic acid (CHCA, %), beta-casein (β-casein, 98%), horseradish peroxidase (HRP, 850 units per mg), bovine serum albumin (BSA, 95%), ammonium bicarbonate (NH_4HCO_3, 99.5%) and TPCK treated trypsin (E.G 2.4.21.4) were purchased from Sigma-Aldrich (St. Louis, MO, USA). Acetonitrile (ACN, 99.9%) and trifluoroacetic acid (TFA, 99.8%) were purchased from Merck (Darmstadt, Germany). Phosphoric acid (85%) was purchased from Shanghai Feida Chemical Reagents Ltd. (Shanghai, China). Deionized water (18.4 Ω cm^{-1}) used for all experiments was obtained from a Milli Q system (Millipore, Bedford, MA).

Preparation of Fe_3O_4@NH_2

Amine-functionalized magnetic nanoparticles were obtained by a one-pot synthesis method.[27] A solution of 1,6-hexanediamine (3.6 g), anhydrous sodium acetate (4 g) and $FeCl_3 \cdot 6H_2O$ (2 g) as a ferric source in glycol (30 mL) was stirred vigorously at room temperature to give a transparent solution. This solution was then transferred into a Teflon-lined autoclave and reacted at 198 °C for 6 h. The magnetite nanoparticles were then rinsed with water and ethanol (2 or 3 times) to effectively remove the solvent and unbound 1,6-hexanediamine, and then dried at 50 °C before characterization and application. During each rinsing step, the nanoparticles were separated from the supernatant by using magnetic force.

Preparation of tryptic digest of standard proteins

β-Casein, HRP, Myo and ASF were each dissolved in 25 mM NH_4HCO_3 at pH 8.0 (1 mg mL^{-1} for each protein) and denatured by boiling for 10 min. Protein solutions were then incubated with trypsin at an enzyme : substrate ratio of 1 : 40 (w/w) for 12 h at 37 °C to produce proteolytic digests, respectively. The digested products were then diluted with 0.1% formic acid to proper concentration and stored at −20 °C for further experiments.

Selective enrichment of phosphopeptides with Fe_3O_4@NH_2

The obtained Fe_3O_4@NH_2 was suspended in deionized water at 20 mg mL^{-1}. Tryptic digests of β-casein, HRP and Myo were dissolved in 100 μL loading buffer (80% ACN containing 1% TFA), then 2 μL Fe_3O_4@NH_2 was added and incubated at room temperature for 1 min. After that, Fe_3O_4@NH_2 with captured phosphopeptides was separated from the mixed solutions by applying an external magnet. The supernatant as flow-through part was collected for the following glycopeptide enrichment. After washing Fe_3O_4@NH_2 with 100 μL loading buffer to remove the nonspecifically adsorbed peptides, the trapped phosphopeptides were eluted with 10 μL 5% $NH_3 \cdot H_2O$ solution. 1 μL of this solution was used for matrix assisted laser desorption ionization-time of flight-mass spectrometry (MALDI TOFMS) analysis with DHB matrix.

Selective enrichment of glycopeptides with Fe_3O_4@NH_2

The flow-through part was collected after phosphopeptide enrichment and the appropriate volume of 2 M NH_4HCO_3 was added to neutralize acids. Then 2 μL Fe_3O_4@NH_2 was added and incubated at room temperature for 1 min. After that, Fe_3O_4@NH_2 with captured glycopeptides was separated from the mixed solutions by applying an external magnet. After washing Fe_3O_4@NH_2 with 100 μL loading buffer to remove the nonspecifically adsorbed peptides, the trapped glycopeptides were eluted with 10 μL CHCA matrix solution, and 1 μL of this solution was used for MALDI TOFMS analysis with CHCA.

MALDI mass spectrometry analysis

MALDI-TOF mass spectrometry analysis was performed in positive reflection mode on a 5800 Proteomic Analyzer (Applied

Biosystems, Framingham, MA, USA) with a Nd:YAG laser at 355 nm, a repetition rate of 400 Hz and an acceleration voltage of 20 kV. The range of laser energy was optimized to obtain good resolution and signal to noise ratio (S/N) and kept constant for further analysis. External mass calibration was performed by using standard peptides from myoglobin digests. At least 1000 laser shots were typically accumulated, whereas in the MS/MS mode spectra up to 2000 laser shots were acquired and averaged. Peptides were fragmented with collision induced decomposition (CID) with an energy of 1 kV.

Results and discussion

Synthesis and characterization of Fe_3O_4@NH_2

The prepared amine-functionalized magnetite nanoparticles were characterized with different methods. The morphology of the as-prepared nanoparticles were characterized by transmission electron microscopy (TEM). Fig. 1a displays a representative image of the Fe_3O_4@NH_2 nanoparticles. The obtained products were dominated by the round shape with an average diameter of *ca.* 25 nm. The TEM images also revealed that the magnetic nanomaterials showed good dispersibility in the solvent, which made them able to capture phosphopeptides or glycopeptides in a short time. The crystalline structure of the Fe_3O_4@NH_2 was rigorously investigated using powder X-ray diffraction (PXRD, Fig. 1b). The Fe_3O_4@NH_2 nanoparticles showed a simple PXRD pattern: eight characteristic peaks for 2θ = 18.07, 29.96, 35.30, 36.92, 42.93, 53.30, 56.83, and 62.38) were observed. These typical peaks correspond to the reflections of (111), (220), (311), (222), (400), (422), (511), and (440) crystalline planes, respectively, which could be well ascribed to the typical cubic structure of Fe_3O_4 (JCPDS 19-629). To provide

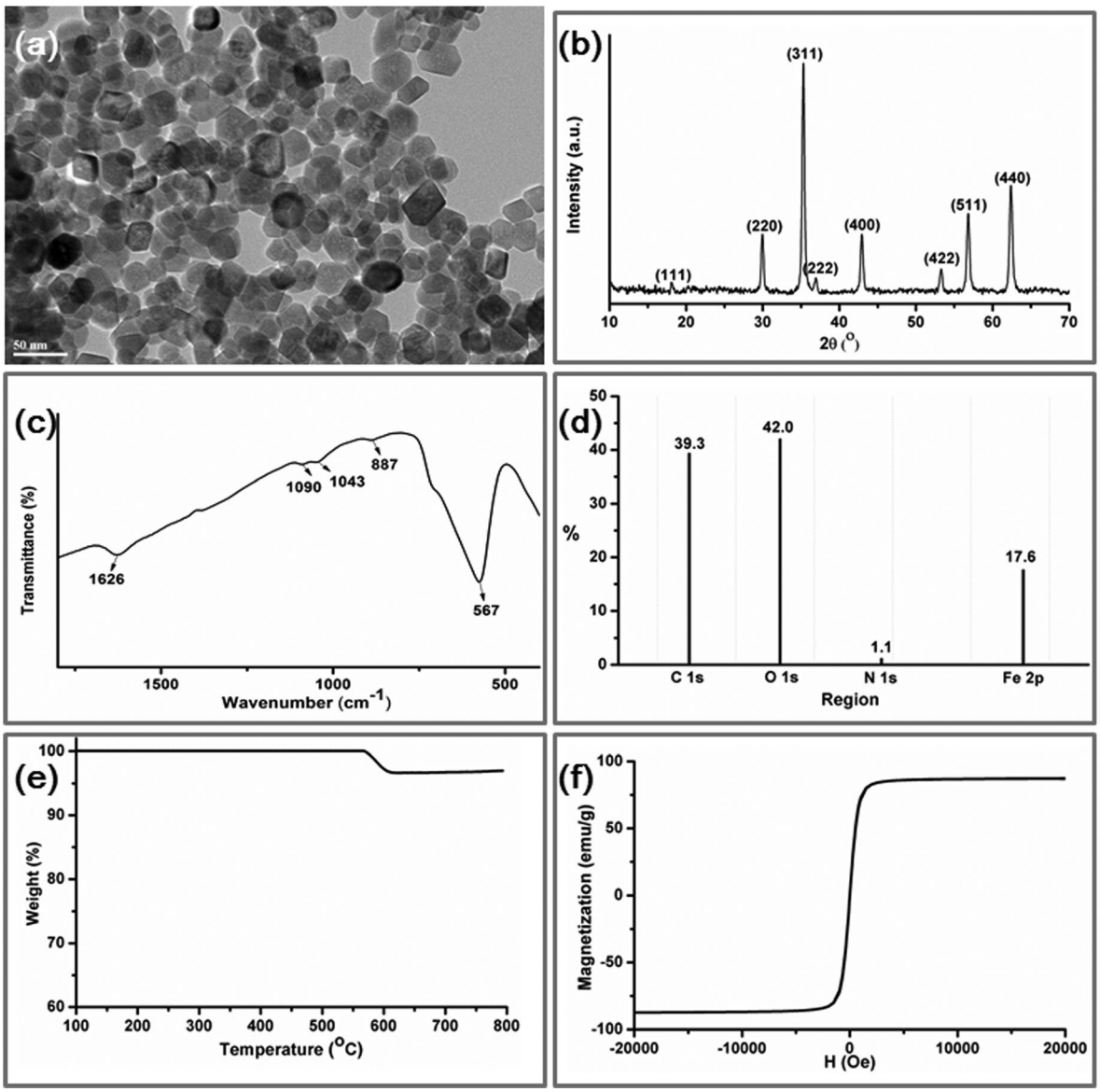

Fig. 1 (a) TEM images; (b) XRD patterns; (c) FT-IR spectra; (d) XPS, (e) TGA curves and (f) magnetic hysteresis curves of Fe_3O_4@NH_2.

direct proof for the amine functionalization, Fourier transform infrared (FTIR) spectroscopy was used to characterize the amine-functionalized magnetite nanoparticles. Fig. 1c shows the IR spectrum of the amine-functionalized magnetic nanoparticles. The strong IR band at 567 cm^{-1} is attributed to the vibration of the Fe–O, while the characteristic peaks around 1626, 1090, 1043 and 887 cm^{-1} matched well with that from free 1,6-hexanediamine, indicating the existence of the free NH_2 group on the amine-functionalized nanomaterials. X-ray photoelectron spectroscopy (XPS) analysis (Fig. 1d) further shows the percentage content for the four main elements of C, O, N and Fe. The 1.1% content of N gives additional evidence for the existence of the surface NH_2 group. Furthermore, thermogravimetric analysis (TGA) was performed to estimate the content of hexanediamine, the weight loss around 600 °C (Fig. 1e) indicates that the content of hexanediamine is as high as 3.1 wt%, which agrees well with the XPS result. Finally, the magnetic properties of the Fe_3O_4@NH_2 were studied using a vibrating sample magnetometer (VSM). The magnetic hysteresis curve of the dried sample at room temperature is illustrated in Fig. 1f, indicating that it possesses a superparamagnetic feature with the saturation magnetization (M_s) value of 87.4 emu g^{-1}. The high M_s value meant that the magnetite nanoparticles could be rapidly separated from the solution (VH_2O/VCH_3CN, 80 : 20) in only 30s when the magnetic field was applied. All of the above characterization clearly proved that the Fe_3O_4@NH_2 was successfully synthesized with the facile one-pot synthesis method.

Sequential enrichment of phosphopeptides and glycopeptides by Fe_3O_4@NH_2

The scope of this study is to develop a new approach for sequentially selective isolation phosphopeptides and glycopeptides, as shown in Scheme 1.

The enrichment efficiency of Fe_3O_4@NH_2 for phosphopeptides and glycopeptides was first investigated using tryptic digests from a phosphoprotein β-casein mixed with a glycoprotein HRP, β-casein and HRP were mixed with a molar ratio of 1 : 1. Fe_3O_4 nanoparticles have been reported as a candidate for the enrichment of phosphopeptides. Phosphopeptides can be captured by Fe_3O_4 through bridging bidentate bonds between the phosphoric acid groups of the phosphopeptides and Fe_3O_4. In addition, the negatively charged phosphate groups on the phosphopeptides also provide a possible means of enriching phosphopeptides by interaction with positively charged objects. At low pH, the amino group was easily protonated and carried a positive charge, because most primary amines were reported with a mean pK_a of 9. The zeta potential of the Fe_3O_4@NH_2 particles in a solution of 80% ACN containing 1% TFA was measured. The results show that the zeta potential of Fe_3O_4@NH_2 was +30 mV in the above-mentioned solution. Therefore, we assume that Fe_3O_4@NH_2 could be an ideal positively charged substrate to capture phosphopeptides in the acidic solution. The combination of the above-mentioned factors would certainly result in a selective enrichment of the phosphopeptides. In the phosphopeptide enrichment procedure, the tryptic digests of β-casein and HRP were first dissolved in 100 μL loading buffer consisting of 80% acetonitrile containing 1% TFA, and then incubated with Fe_3O_4@NH_2 for about 1 min with ultrasonication. After that, the Fe_3O_4@NH_2 with captured phosphopeptides was separated from the mixed solution, using an external magnetic field. The collected products were then washed with the loading buffer to remove non-specifically adsorbed peptides. Finally, the trapped phosphopeptides were eluted with 10 μL 5% $NH_3 \cdot H_2O$, and 1 μL of this solution was used for MALDI TOFMS analysis. Fig. 2a and 2b present mass spectra of tryptic digests of a mixture of β-casein and HRP without enrichment, obtained with DHB and CHCA matrix, respectively.

The spectrum, either Fig. 2a or 2b, is dominated by non-phosphopeptides, and their presence led to a low signal to noise ratio for the phosphopeptides. After selective enrichment, signals could be clearly observed for all of the three phosphopeptides (at *m/z* 2061.83, *m/z* 2556.09, and *m/z* 3122.27) along with their doubly charged phosphorylated peptides, without any interference of nonphosphopeptides, as shown in Fig. 2c. We also notice that both mono-phosphopeptides (*m/z* 2061.83 with one phosphorylation site) and multi-phosphopeptides (*m/z* 3122.27 with four phosphorylation sites) are observed, which shows the good enrichment ability of Fe_3O_4@NH_2 for different types of phosphopeptides.

In order to capture glycopeptides, the flow-through part after phosphopeptide enrichment was collected. Among various enrichment methods, HILIC-based enrichment methods have drawn increasing attention in recent years. HILIC-based methods have shown broad glycan specificity and good compatibility with MS analysis. A variety of hydrophilic matrices including sepharose,[28] cellulose,[29] click maltose-HILIC,[30] and amide-based stationary phases[31,32] have been developed for the enrichment of glycopeptides. It is reasoned that glycopeptides would be bound more strongly than nonglycosylated ones on NH_2-functionalized magnetic nanoparticles *via* hydrophilic interactions due to the additional contribution of the hydrophilic glycan moiety. Furthermore, the working principle relying on the fact that glycopeptides are, in general, more hydrophilic than non-glycosylated peptides, makes the whole enrichment nonselectively capture a full range of glycopeptides irrespective of the attached glycan structures. In order to enrich glycopeptides, the collected solution should be adjusted making the hydrophilic interaction play a dominant role for glycopeptide enrichment.

Different volumes of 2 M NH_4HCO_3 solution were added. Finally, 6 μL of 2 M NH_4HCO_3 solution was added to neutralize the acid. After addition of NH_4HCO_3, the ultimate pH was close to 7.2. Then 2 μL of Fe_3O_4@NH_2 was added and incubated for

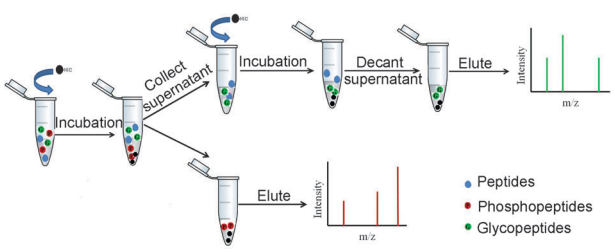

Scheme 1 Workflow of the sequential enrichment strategy for phosphopeptides and glycopeptides by Fe_3O_4@NH_2.

about 1 min with ultrasonication. After that, the Fe_3O_4@NH_2 with captured glycopeptides was separated from the mixed solution, using an external magnetic field. The collected products were washed with the loading buffer, to remove nonspecifically adsorbed peptides. Finally, the trapped glycopeptides were eluted with 10 μL CHCA matrix solution, and 1 μL of this solution was used for MALDI TOFMS analysis. After selective enrichment, all of the five glycopeptides (at *m*/*z* 3353.40, *m*/*z* 3671.70, *m*/*z* 3895.66, *m*/*z* 4222.47 and *m*/*z* 4985.18) could be clearly observed without the interference of nonglycopeptides, as shown in Fig. 2d. This result thus confirmed the selectivity of Fe_3O_4@NH_2 for glycopeptides.

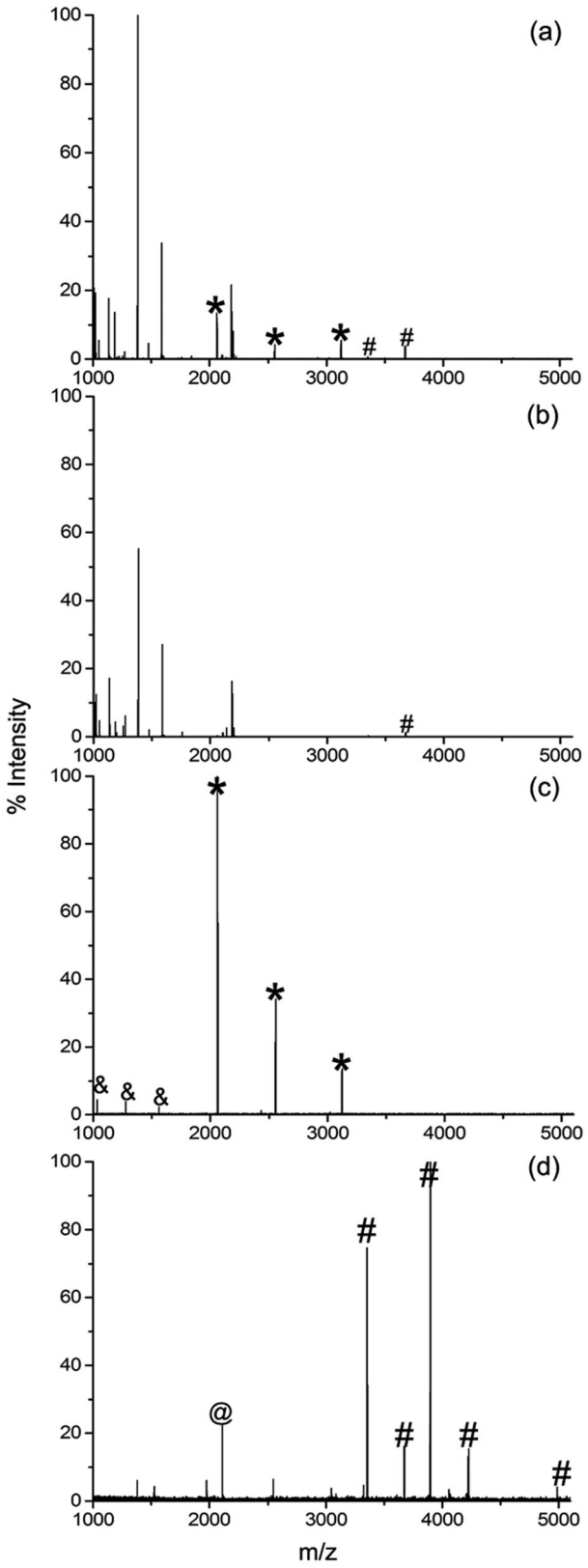

To demonstrate the feasibility of the sequential enrichment strategy in handling complex mixtures, a relatively complex peptide mixture of tryptic digests of β-casein : HRP : Myo with a molar ratio of 1 : 1 : 10 was investigated. As shown in Fig. 3a and b, phosphopeptides and glycopeptides were difficult to distinguish before enrichment, due to the presence of large amounts of nonphosphopeptides and nonglycopeptides from the Myo digests. After incubation with Fe_3O_4@NH_2, all of the three phosphopeptides could be easily detected, with a very clean background in the mass spectrum (Fig. 3c) and five glycopeptides could also be detected (Fig. 3d). A comparison between the amino-functionalized magnetic nanoparticles and magnetic nanoparticles without amino groups for their adsorption was performed (Fig. 4). Although phosphopeptides can be selectively enriched from the peptide mixture with bare Fe_3O_4, the selectivity is lower than that of Fe_3O_4@NH_2, because peptides from Myo digests still can be detected with low intensity (Fig. 4a), and the multi-phosphopeptides *m*/*z* 3122 cannot be detected.

Glycopeptides cannot be selectively enriched effectively from the flow-through part after phosphopeptide enrichment. Therefore, we assume that the amino groups on the nanoparticles were important for the enrichment of the glycopeptides (Fig. 4b).

The detection sensitivity of phosphopeptides and glycopeptides using Fe_3O_4@NH_2 nanoparticles was studied. Even at a low concentration of 1.0 nM (100 μL), corresponding to 100 fmol β-casein, phosphopeptides were still observed after enrichment (Fig. 5a). With the same method, the detection limit of glycopeptides was determined as 5.0 nM (100 μL), corresponding to 500 fmol HRP, shown in Fig. 5b. The post enrichment recovery of phosphopeptides from Fe_3O_4@NH_2 was also investigated. A certain amount of standard β-casein or HRP digests was divided equally into two parts. The first part was treated with immobilized trypsin (homemade) in $H_2{}^{18}O$, which produced a 4 Da mass increase by introducing two ^{18}O atoms at the C termini of the peptides. The second part was applied in our trap and release strategy. By mixing the two parts, we could profile the product by MS to make a comparative study of the abundances of the phosphopeptides/glycopeptides from different oxygen isotopes, according to the peak relative intensities. The recovery of phosphopeptides and glycopeptides are calculated to be 88% and 76%, respectively.

Fig. 2 MALDI mass spectra of the tryptic digest mixture of β-casein and HRP (with a molar ratio of β-casein to HRP of 1 : 1). (a) Direct analysis with DHB matrix, (b) direct analysis with CHCA matrix, (c) eluate from Fe_3O_4@NH_2 after phosphopeptides enrichment and (d) eluate from Fe_3O_4@NH_2 after glycopeptide enrichment using glycopeptides was enriched from the flow-through part after phosphopeptide enrichment. ''*'' and ''&'' indicate phosphopeptides and their doubly charged form, ''#'' and ''@'' indicate glycopeptides and their doubly charged form.

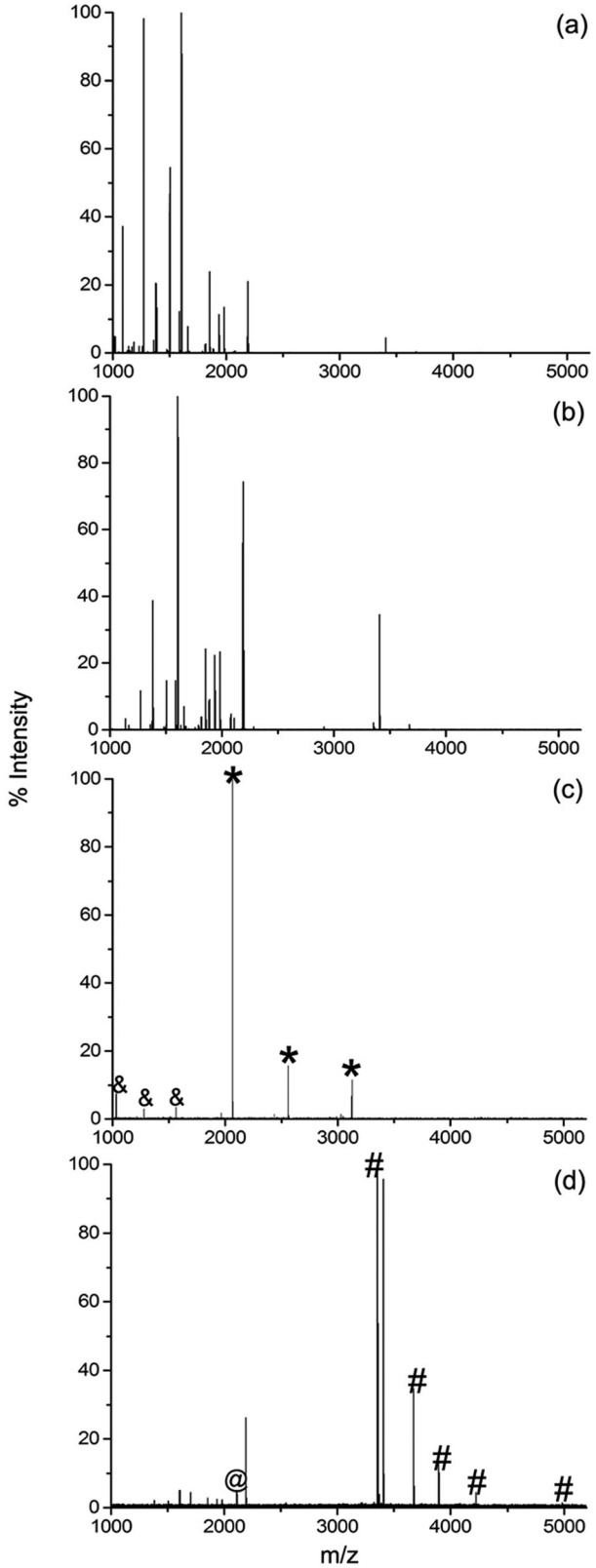

Fig. 3 MALDI mass spectra of the tryptic digest mixture of β-casein, HRP and Myo (with a molar ratio of β-casein : HRP : Myo of 1 : 1 : 10). (a) Direct analysis with DHB matrix, (b) direct analysis with CHCA matrix, (c) eluate from Fe_3O_4@NH_2 after phosphopeptide enrichment (d) eluate from Fe_3O_4@NH_2 after glycopeptide enrichment; glycopeptides were enriched from the flow-through part after phosphopeptide enrichment. ''*'' and ''&'' indicate phosphopeptides and their doubly charged form, ''#'' and ''@'' indicate glycopeptides and their doubly charged form.

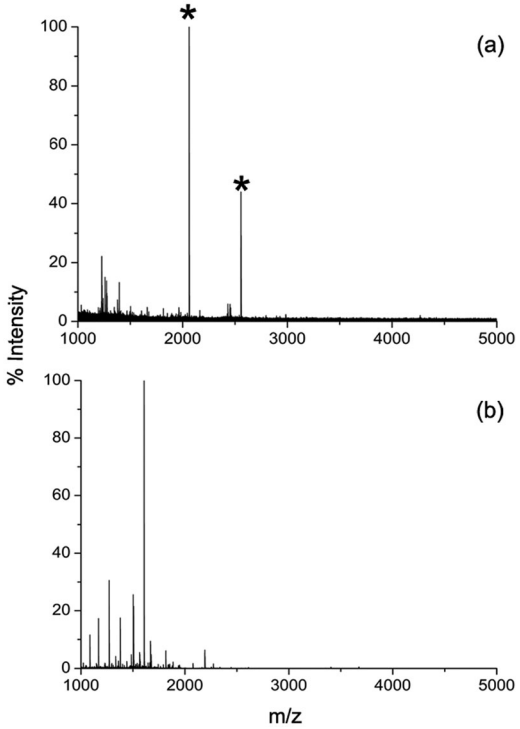

Fig. 4 MALDI mass spectra of the tryptic digest mixture of Myo, β-casein and HRP (with a mass ratio of Myo : β-casein : HRP of 10 : 1 : 1). (a) Eluate from Fe_3O_4 after phosphopeptide enrichment and (b) eluate from Fe_3O_4 after glycopeptide enrichment. ''*'' indicates phosphopeptides.

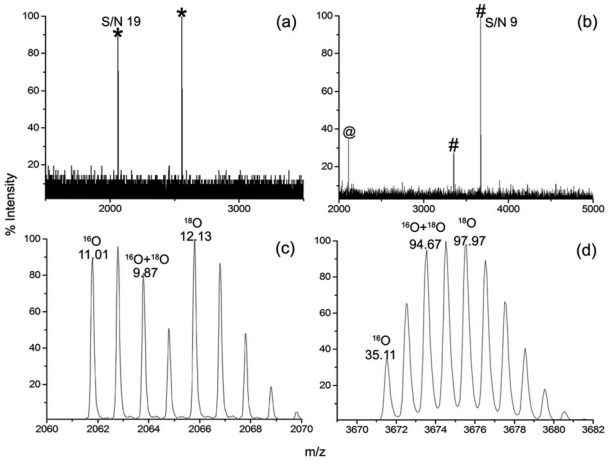

Fig. 5 MALDI mass spectra of (a) the enriched eluate of a tryptic digest of β-casein (1.0 nM, 100 μL); (b) the enriched eluate of a tryptic digest of HRP (5.0 nM, 100 μL); (c) β-casein (a mixture of unlabeled enriched and an equal amount of ^{18}O labeled unenriched, used as a control); (d) HRP (a mixture of unlabeled enriched and an equal amount of ^{18}O labeled unenriched, used as a control).

Analysis of phosphopeptides and glycopeptides of ASF by Fe_3O_4@NH_2 enrichment

ASF, a glycoprotein with potential phosphorylation sites was chosen as a model to further test this sequential enrichment method. Fig. 6a and b present mass spectra of tryptic digests ASF without enrichment obtained with DHB and CHCA

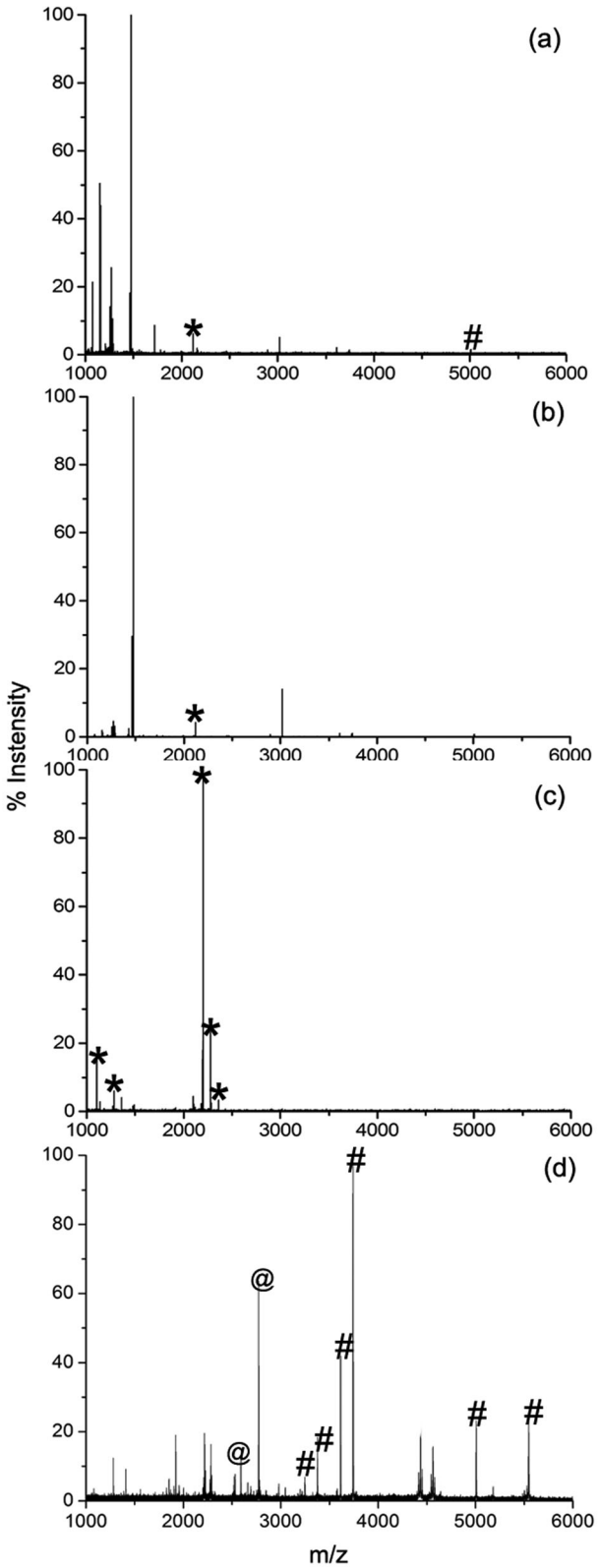

Fig. 6 MALDI mass spectra of the tryptic digest ASF. (a) Direct analysis with DHB matrix, (b) direct analysis with CHCA matrix, (c) eluate from Fe_3O_4@NH_2 after phosphopeptide enrichment and (d) eluate from Fe_3O_4@NH_2 glycopeptides after enrichment. ''*'' Indicates phosphopeptides, ''#'' and ''@'' indicate glycopeptides and their doubly charged form.

matrixes, respectively. Before enrichment, nonphosphopeptides and nonglycopeptides dominate in the spectrum: only one phosphopeptide and one glycopeptide can be detected. Fig. 6c shows the mass spectrum after phosphopeptide enrichment; signals at *m*/*z* 1280.59, 1360.59, 2199.90, 2279.86, and *m*/*z* 2359.81 were easily detected with a very clean background.

Tandem MS was performed to confirm their phosphorylation site. Taking *m*/*z* 2199.90 as example, loss of phosphoric acid groups from the precursor ion were apparent in the mass spectrum due to collisional activation in the high-pressure zone of the MALDI source, indicating the presence of a phosphorylation (data not shown). Fig. 7 is a magnification of the tandem mass spectrum. Fragment ions that were evident in the spectrum were the C-terminal y8–y15 ions for the phosphopeptide. It was possible to confirm the known amino acid sequence and to localize the phosphorylation sites. The mass difference between y10 and y11 clearly indicated that the phosphorylation is located at the position of serine 323 in the peptide HTFSGVASVEpSSSGEAFHVGK. Similarly, phosphorylation sites at S_{134}, S_{138}, S_{316}, S_{323}, S_{325} were also confirmed by MS/MS analysis, respectively. The details of detected phosphopeptides and their modification sites are listed in Table 1. For the first time, the phosphorylation sites of ASF from bovine were proved by experiment. Fig. 6d shows that, after glycopeptide enrichment, signals of *m*/*z* 3247.24(N_{156}), *m*/*z* 3375.32(N_{156}), *m*/*z* 3612.37(N_{156}) *m*/*z* 3740.46(N_{156}), 5005.11(N_{176}) and *m*/*z* 5544.31(N_{99}) were detected, from the corresponding glycopeptides from the three known glycosites at asparagine 99, 156 and 176. We also noticed that the sequence coverage of ASF was increased from 25.6% to 51.8% corresponding to a 102% increase when counting the phosphopeptides and glycopeptides in.

Conclusion

In summary, we have developed a feasible method for sequential enrichment of phosphopeptides and glycopeptides with amine-functionalized magnetic nanoparticles. The sequential enrichment strategy allowed phosphopeptides and glycopeptides to be sensitively and selectively analyzed in one experiment. In addition, the high magnetic susceptibility of the magnetic nanoparticles allowed

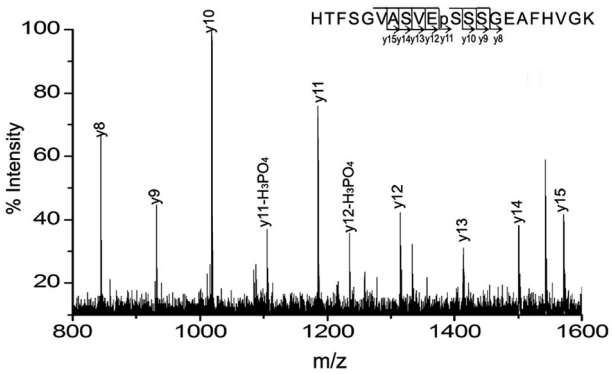

Fig. 7 Representative MS/MS spectrum of phosphopeptide HTFSGVASVEpSSSGEAFHVGK.

Table 1 Overview of observed phosphopeptides and glycopeptides derived from tryptic digests of ASF after enrichment with Fe_3O_4@NH_2. ''N#'' denotes the N-linked glycosylation site

Observed *m/z*	Sequence	Modification site
1280.59	CDpSSPDSAEDVR	134
1360.59	CDpSSPDpSAEDVR	134, 138
2199.90	HTFSGVASVEpSSSGEAFHVGK	323
2279.86	HTFSGVASVEpSSpSGEAFHVGK	323, 325
2359.81	HTFpSGVASVEpSSpSGEAFHVGK	316, 323, 325

Observed *m/z*	Sequence	Glycan composition	Modification site
3247.24	KLCPDCPLLAPLN#DSR	$GlcNAc_3GlcNAc$(Partial) $Man_3GlcNAc_2$	156
3375.32	RKLCPDCPLLAPLN#DSR	$GlcNAc_3GlcNAc$(Partial) $Man_3GlcNAc_2$	156
3612.37	KLCPDCPLLAPLN#DSR	$GlcNAc_4GlcNAc$(Partial) Man $Man_3GlcNAc_2$	176
3740.46	RKLCPDCPLLAPLN#DSR	$GlcNAc_4GlcNAc$(Partial) Man $Man_3GlcNAc_2$	176
5005.11	VVHAVEVALATFNAES N#GSYLQLVEISR	$Gal_3GlcNAc_3Man_3GlcNAc_2$	99
5544.31	RPTGEVYDIEIDTLETCHVLDPTPLAN#CSVR	$Gal_3GlcNAc_3Man_3GlcNAc_2$	99

convenient separation of the target peptides by magnetic separation, thus the whole enrichment procedure was completed in a very short period. Therefore, this sequential enrichment method not only increases the overall detection sensitivity but also saves the whole sample pretreatment time. We believe that this is a very promising technology for the highly specific analysis of phosphopeptides and glycopeptides simultaneously.

Acknowledgements

The work was supported by NST (2012CB910602, 2012AA020203, 2012CB910103 and 2012YQ12004409), NSF (21025519 and 21005020, 31070732), Shanghai Projects (11XD1400800, B109 and 20114Y167) and Fundamental Research Funds for the Central Universities.

References

1 G. A. Khoury, R. C. Baliban and C. A. Floudas, *Sci. Rep.*, 2011, 1.
2 M. B. Yaffe, *Nat. Rev. Mol. Cell Biol.*, 2002, **3**, 177–186.
3 A. Varki, J. D. Esko and K. J. Colley, in *Essentials of Glycobiology*, ed. A. Varki, R. D. Cummings, J. D. Esko, H. H. Freeze, P. Stanley, C. R. Bertozzi, G. W. Hart and M. E. Etzler, Cold Spring Harbor, NY, 2nd edn, 2009.
4 R. Wu, W. Haas, N. Dephoure, E. L. Huttlin, B. Zhai, M. E. Sowa and S. P. Gygi, *Nat. Methods*, 2011, **8**, 677–683.
5 D. F. Zielinska, F. Gnad, J. R. Wisniewski and M. Mann, *Cell*, 2010, **141**, 897–907.
6 A. Doerr, *Nat. Methods*, 2012, **9**, 36.
7 H. Zhang, P. Loriaux, J. Eng, D. Campbell, A. Keller, P. Moss, R. Bonneau, N. Zhang, Y. Zhou, B. Wollscheid, K. Cooke, E. C. Yi, H. Lee, E. R. Peskind, J. Zhang, R. D. Smith and R. Aebersold, *Genome Biol.*, 2006, **7**, R73.
8 M. J. Chalmers, W. Kolch, M. R. Emmett, A. G. Marshall and H. Mischak, *J. Chromatogr., B: Anal. Technol. Biomed. Life Sci.*, 2004, **803**, 111–120.
9 T. E. Thingholm, O. N. Jensen and M. R. Larsen, *Proteomics*, 2009, **9**, 1451–1468.
10 B. Xu, L. Zhou, F. Wang, H. Qin, J. Zhu and H. Zou, *Chem. Commun.*, 2012, **48**, 1802–1804.
11 D. Qi, Y. Mao, J. Lu, C. Deng and X. Zhang, *J. Chromatogr., A*, 2010, **1217**, 2606–2617.
12 C. Pan, M. Ye, Y. Liu, S. Feng, X. Jiang, G. Han, J. Zhu and H. Zou, *J. Proteome Res.*, 2006, **5**, 3114–3124.
13 W. F. Ma, Y. Zhang, L. L. Li, L. J. You, P. Zhang, Y. T. Zhang, J. M. Li, M. Yu, J. Guo, H. J. Lu and C. C. Wang, *ACS Nano*, 2012, **6**, 3179–3188.
14 H. K. Kweon and K. Hakansson, *Anal. Chem.*, 2006, **78**, 1743–1749.
15 Y. Li, Y. Liu, J. Tang, H. Lin, N. Yao, X. Shen, C. Deng, P. Yang and X. Zhang, *J. Chromatogr., A*, 2007, **1172**, 57–71.
16 A. Lee, H. J. Yang, E. S. Lim, J. Kim and Y. Kim, *Rapid Commun. Mass Spectrom.*, 2008, **22**, 2561–2564.
17 C. K. Chang, C. C. Wu, Y. S. Wang and H. C. Chang, *Anal. Chem.*, 2008, **80**, 3791–3797.
18 C. T. Chen, L. Y. Wang and Y. P. Ho, *Anal. Bioanal. Chem.*, 2011, **399**, 2795–2806.
19 M. Gronborg, *Mol. Cell. Proteomics*, 2002, **1**, 517–527.
20 H. Zhou, J. D. Watts and R. Aebersold, *Nat. Biotechnol.*, 2001, **19**, 375–378.
21 R. R. Drake, E. E. Schwegler, G. Malik, J. Diaz, T. Block, A. Mehta and O. J. Semmes, *Mol. Cell. Proteomics*, 2006, **5**, 1957–1967.
22 Y. Tian, Y. Zhou, S. Elliott, R. Aebersold and H. Zhang, *Nat. Protoc.*, 2007, **2**, 334–339.
23 Y. Xu, Z. Wu, L. Zhang, H. Lu, P. Yang, P. A. Webley and D. Zhao, *Anal. Chem.*, 2009, **81**, 503–508.
24 J. Yan, X. Li, L. Yu, Y. Jin, X. Zhang, X. Xue, Y. Ke and X. Liang, *Chem. Commun.*, 2010, **46**, 5488–5490.
25 R. Apweiler, H. Hermjakob and N. Sharon, *Biochim. Biophys. Acta*, 1999, **1473**, 4–8.
26 J. V. Olsen, M. Vermeulen, A. Santamaria, C. Kumar, M. L. Miller, L. J. Jensen, F. Gnad, J. Cox, T. S. Jensen, E. A. Nigg, S. Brunak and M. Mann, *Sci. Signaling*, 2010, **3**, ra3.

27 L. Wang, J. Bao, F. Zhang and Y. Li, *Chemistry*, 2006, **12**, 6341–6347.
28 Y. Wada, M. Tajiri and S. Yoshida, *Anal. Chem.*, 2004, **76**, 6560–6565.
29 S. I. Snovida, E. D. Bodnar, R. Viner, J. Saba and H. Perreault, *Carbohydr. Res.*, 2010, **345**, 792–801.
30 S. Mysling, G. Palmisano, P. Hojrup and M. Thaysen-Andersen, *Anal. Chem.*, 2010, **82**, 5598–5609.
31 M. Wuhrer, C. A. Koeleman, C. H. Hokke and A. M. Deelder, *Anal. Chem.*, 2005, **77**, 886–894.
32 C. W. Kuo, I. L. Wu, H. H. Hsiao and K. H. Khoo, *Anal. Bioanal. Chem.*, 2012, **402**, 2765–2776.

